Towards clinical implementation of quantitative PET and SPECT imaging

Burgt, A. van de

CHAPTER 4

[^{18}F]FDG administered activity reduction capabilities of a 32-cm axial field-of-view solid-state digital bismuth germanium oxide PET/CT system while maintaining EARL compliance

Authors
A. van de Burgt, P. Dibbets-Schneider, F. Kotasidis, L.F. de Geus-Oei, D.D.D. Rietbergen and F.H.P. van Velden

Published
Physica Medica, 2025; 131: 104935,
DOI: 10.1016/j.ejmp.2025.104935

Supplementary materials
https://doi.org/10.1016/j.ejmp.2025.104935

ABSTRACT

Purpose

To assess the lower [^{18}F]FDG limit in administered activity and/or scan time reduction capabilities of a digital-BGO 32-cm axial field-of-view PET system while being compliant with current and updated EANM Research Ltd Fluorine-18 accreditation specifications ($EARL_1$ and $EARL_2$).

Methods

$EARL_1$ and $EARL_2$ compliance of the digital-BGO system (Omni Legend 32 cm) was tested for several reconstructions, including those that apply precision deep learning-based image enhancement (PDL) as postprocessing, using the calibration QC and NEMA IEC phantom measurements. The image quality QC scan was repeated every hour for 7 hours, with each subsequent hour representing a lower administered activity, and reconstructed for various times per bed position, i.e. 30, 60, 120, 180, and 300 seconds. For each of the image quality QC images, coefficient of variation (COV) of the background compartment, and mean, maximum and peak activity concentration recovery coefficients (RC_{mean}, RC_{max} and RC_{peak}) of differently-sized spheres were calculated and compared to current and updated EARL accreditation specifications.

Results

When we apply 1 min per bed position for PET acquisition, [^{18}F]FDG administration can be reduced by a factor of ~4 for $EARL_1$, by a factor of ~8 for $EARL_2$ (2 mm voxels) and by a factor of ~4 for $EARL_2$ (4 mm voxels) using both standard reconstructions and PDL post-processing compared to current EANM recommendations for [^{18}F]FDG administration (7 $MBq \cdot min \cdot bed^{-1} \cdot kg^{-1}$).

Conclusions

Reduction in [^{18}F]FDG administered activity is possible by at least a factor 4 for 1 min/bed with the Omni Legend 32 cm PET/CT while maintaining $EARL_1$ and $EARL_2$ compliance.

Keywords

Administered activity reduction; scan time reduction; PET/CT; EARL ^{18}F accreditation; phantom study; [^{18}F]FDG

4

INTRODUCTION

Positron emission tomography/computed tomography (PET/CT) imaging is a powerful tool that enables whole body non-invasive visualization and quantification of biological processes at the molecular level [1]. Continuous advancements in PET/CT technology have led to improved image quality and increased sensitivity, thereby potentially enhancing diagnostic accuracy which may lead to better patient outcomes [2]. Recently, a digital PET/CT with bismuth germanium oxide scintillating crystals coupled to silicon photomultipliers (SiPM) over an extended 32 cm axial field-of-view (FOV) was introduced (Omni Legend; GE HealthCare, Milwaukee, USA). This novel non-time-of-flight PET/CT system demonstrates high count rates (peak noise-equivalent count rates: ~500 kcps) and a superior sensitivity (45-49 cps/kBq) according to the National Electric Manufacturer's Association (NEMA) NU2-2018 standard [3], while maintaining a spatial resolution comparable to other current SiPM-based time-of-flight PET/CT systems [4-6]. Moreover, it incorporates precision deep learning-based image enhancement (PDL) that aims to provide improved feature sharpness and convergence comparable to hardware-based time-of-flight reconstruction [7]. The enhanced sensitivity of the system provides possibilities to reduce both scan duration and/or the administered activity of radiopharmaceuticals. Shorter scan durations may enhance patient comfort, increase patient throughput and decrease the risk of patient motion. Lowering the administered activity offers opportunities for cost savings and reduces the risks associated with radiation exposure for both staff and patients [5]. Kennedy et al. briefly highlighted the potential to reduce administered activity and scan time of the Omni legend PET/CT system for various radiotracers and injected activities [5], but a thorough investigation into the administered activity and/or scan time reduction capabilities of this new system has not yet been conducted. This study aims to assess the lower limit in administered activity of 2-deoxy-2-[^{18}F]fluoro-D-glucose ([^{18}F]FDG) and/or scan time reduction capabilities for the Omni Legend PET/CT while being compliant with current and updated European Association of Nuclear Medicine (EANM) Research Ltd Fluorine-18 accreditation specifications ($EARL_1$ and $EARL_2$).

MATERIAL AND METHODS

$EARL_1$ and $EARL_2$ compliance of the Omni Legend system was tested using calibration QC and NEMA IEC phantom measurements [8-11].

Phantom studies

All PET acquisitions covered two bed positions with a 47% bed overlap and were performed on an EARL ^{18}F standards 1 and 2 accredited PET/CT system (Omni Legend 32 cm, GE Healthcare, Milwaukee, USA) [8, 9]. Prior to each PET scan, a low-dose CT scan (120 kVp, 52 mAs, with dose modulation) was acquired for attenuation correction purposes.

For the calibration QC scan, a cylindrical uniformity phantom with a diameter of 20 cm and a length of 30 cm was filled with distilled water and 82.2 MBq of [^{18}F]FDG, and placed in the centre of the FOV. A PET scan was acquired in list-mode for 5 min per bed position.

For assessing the system-specific patient [^{18}F]FDG activity using image quality QC scans, a NEMA IEC body phantom, equipped with six fillable spheres varying in diameter (10, 13, 17, 22, 28, and 37 mm) and a lung insert, was filled with distilled water, and 2.39 kBq/mL (uniform background compartment) and 22.6 kBq/mL (spheres) of [^{18}F]FDG, simulating a sphere to background ratio of ~10:1. The spheres of the phantom were positioned in the centre of the FOV. A PET scan was acquired in list-mode for 10 min per bed position (T0), and repeated every hour for 7 hours (T0+1h to T0+7h), with each subsequent hour representing a lower activity. Boellaard et al described the entire procedure for assessing system-specific patient [^{18}F]FDG activity preparations for quantitative [^{18}F]FDG PET/CT studies [10].

More details for preparation and acquisition requirements of EARL fluor-18 accreditation can be found in the EARL standard operating procedures [11].

PET reconstructions

The list-mode data of the PET scan of the calibration QC were histogrammed into sinograms of 300 seconds per bed position, while the list-mode data of each PET scan (T0 till T0+7h) of the image quality QC were histogrammed into sinograms of 30, 60, 120, 180, and 300 seconds per bed position. The 300 seconds per bed position of T0 was used to validate the image quality of the reconstructions to be $EARL_1$ or $EARL_2$ compliant. The following five reconstructions were performed:

- $EARL_1$ images were reconstructed using a 3D maximum likelihood ordered subset expectation maximization reconstruction (3D OSEM) (VUEPointHD (VPHD)) with 4 iterations and 12 subsets, followed by a 7 mm full-width-at-half-maximum (FWHM)

Gaussian filter and a 192x192 matrix, resulting in a voxel size of 3.65 x 3.65 x 2.07 mm^3 (1).

- $EARL_2$ 2 mm images were reconstructed using a Bayesian penalised likelihood reconstruction (BPL; Q.Clear) with a β parameter of 1500 and a 384x384 matrix, resulting in 1.82 x 1.82 x 2.07 mm^3 voxels (2), and repeated with PDL post-processing using a 'low' level of contrast-enhancement (3).
- $EARL_2$ 4 mm images were reconstructed using BPL with a β parameter of 1200 and a 192 x 192 matrix, resulting in 3.65 x 3.65 x 2.07 mm^3 voxels (4), and repeated with the 'low' level of PDL post-processing (5).

All reconstructions were performed with corrections for attenuation, scatter, normalization, decay, and dead time. For each of the image quality QC images, coefficient of variation (COV) of the background compartment, and mean, maximum and peak activity concentration recovery coefficients (RC_{mean}, RC_{max} and RC_{peak}) of differently-sized spheres were calculated and compared to current and updated EARL accreditation specifications [8, 10, 12].

Data analysis

For each PET image of the calibration QC, the average volumetric standardized uptake value (SUV) bias, which cannot exceed 10%, is calculated by:

$$SUV_{bias}(\%) = \left(\frac{C_{measured}}{C_{calculated}} - 1\right) \times 100\% \qquad (1)$$

In this equation $C_{measured}$ represents the activity concentration measured from images and $C_{calculated}$ is the true activity concentration calculated from injection data. The SUV_{bias} was generated using the manual tool implemented in IDL (version 8.4; Harris Geospatial Solutions, Bloomfield, USA) by Boellaard et al [8, 12]. Maximum, peak and mean SUV recovery coefficients (RC_{max}, RC_{mean} and RC_{peak}) were computed for all spheres on each reconstructed PET image quality QC images using an in-house-developed algorithm in MATLAB (version 2018b; MathWorks, Massachusetts, USA), cross-validated with the aforementioned manual tool implemented in IDL by Boellaard et al [8, 12], with a deviation of <1%. In short, this in-house-developed algorithm in MATLAB, using the known geometry of the NEMA IEC body phantom, locates the centroids of the spheres from the PET image and draws volumes of interest (VOIs) on the six spheres together with 3 cm rectangular VOIs (n=9) at predetermined locations (relative to the sphere location and depending on the sphere orientation and position) in the background compartment of the phantom (Figure 1), onto each reconstructed PET image. To limit the effects of partial voxels, using the known sphere diameter, a raster of sample points is created every 0.1 mm and the values are interpolate in these 0.1 locations, thereby creating a finer sampling than the original voxels. For each sphere, the max and peak values are obtained (for the calculation of RC_{max} and RC_{peak}) from the original PET images, and a VOI is created by a 50% background-corrected isocontour method to derive the mean value for the calculation of RC_{mean}. The RC values are calculated by:

$$RC = \frac{S_{measured}}{S_{calculated}} \tag{2}$$

In this equation $S_{measured}$ represents the max, peak or mean activity concentration measured from the VOIs of each sphere and $S_{calculated}$ is the true activity concentration calculated from injection data for the spheres. The obtained RC values should comply to the $EARL_1$ (RC_{max} and RC_{mean}) and $EARL_2$ (also includes RC_{peak}) accreditation specifications [11]. In addition, the coefficient of variation (COV), determined by dividing the standard deviation by the mean of the pixel values within a VOI, was initially computed for each individual 3 cm rectangular VOIs placed in the background compartment (n=9). Subsequently, the final COV parameter was obtained by averaging these 9 COV values. It was essential that the resulting average COV remained below 15% [10].

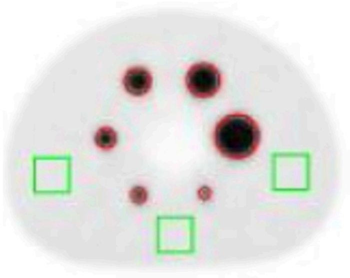

Figure 1. Visualization of the template of the NEMA IEC body phantom geometry used by the in-house-developed algorithm, showing the volumes-of-interest (VOIs) of the six spheres identified on the PET image (red circles) and the rectangular background VOIs (3 cm, n=9, green squares) in axial view.

RESULTS

$EARL_1$ and $EARL_2$ compliance

The calibration QC revealed a median SUV bias of 1.16% (range: 0.40—1.55%). RC_{max}, RC_{mean} and (when applicable) RC_{peak} of all tested reconstructions were $EARL_1$ or $EARL_2$ compliant (Figure 2 and Supplemental file S1).

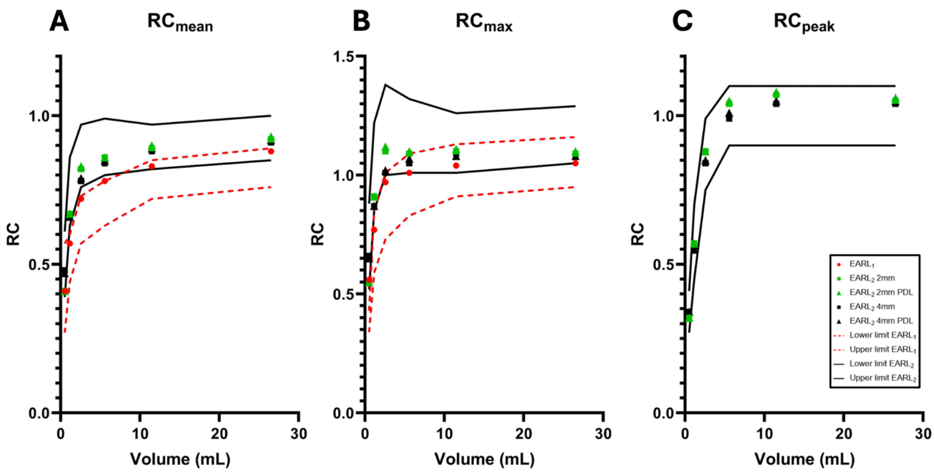

Figure 2. Max (A), mean (B) and peak (C; only $EARL_2$) recovery coefficients (RC) as a function of volume (mL), derived from the image quality QC scan acquired at T0, using 300 seconds per bed position. PDL: precision deep learning image enhancement.

Administered activity and/or scan time reduction capabilities

When we apply 1 min per bed position for PET acquisition, [^{18}F]FDG administration can be reduced by a factor of ~4 for $EARL_1$, by a factor of ~8 for $EARL_2$ (2 mm) and by a factor of ~4 for $EARL_2$ (4 mm) using both standard reconstructions (Figure 3A) and PDL post-processing (Figure 3B) compared to current EANM recommendations for FDG administration (7 MBq·min·bed^{-1}·kg^{-1} of [^{18}F]FDG for a 75 kg patient [9]). This indicates a decrease in MBq/kg for the used reconstructions to 1.75 MBq/kg, 0.88MBq/kg and 1.75 MBq/kg, respectively. $EARL_2$ reconstructions (2 mm and 4 mm voxels) both with and without PDL allowed similar reductions in administered activity, with lower COV values for with PDL (maximum COV difference: 5.2% for 2 mm and 16.5% for 4 mm). Due to the higher beta value applied for $EARL_2$ 2 mm, $EARL_2$ 4 mm voxel size has generally higher COVs than 2 mm, contrary to the expectation of smaller voxels exhibiting higher noise and COV (maximum COV difference: 32.4% with PDL and 45.5% without PDL).

A No PDL	Activity (MBq/kg)	Time per bed position (s) EARL₁					EARL₂ 2mm					EARL₂ 4mm				
		30	60	120	180	300	30	60	120	180	300	30	60	120	180	300
T0	4	12.6	9.7	7.9	6.2	3.9	9.6	6.7	4.9	3.6	2.6	11.3	8.5	5.9	4.1	3.2
T0 + 1h	2.73	17.1	12.4	8.6	6.8	4.1	10.2	7.7	4.4	3.6	2.7	13.4	8.6	5.7	4.3	3.5
T0 + 2h	1.87	19.2	13.6	11.1	7.6	5.7	10.6	8.9	6.2	5.3	3.8	15.4	11.0	7.7	5.9	4.3
T0 + 3h	1.29	24.1	17.4	12.6	9.9	8.0	17.6	10.3	7.1	5.8	5.1	24.2	13.9	9.2	6.9	5.7
T0 + 4h	0.88	25.3	18.2	12.7	11.0	8.8	18.3	12.6	8.0	6.5	5.0	30.5	16.8	9.6	7.9	5.7
T0 + 5h	0.56	30.2	20.3	19.2	16.3	10.9	25.0	15.4	12.8	10.0	7.0	44.4	21.3	16.7	12.6	8.9
T0 + 6h	0.41	32.7	27.3	20.7	16.5	13.1	28.8	21.7	11.6	9.8	8.2	58.3	37.9	18.8	12.8	10.0
T0 + 7h	0.28	36.5	30.5	20.5	16.8	15.1	40.7	24.3	15.1	11.7	9.9	86.2	52.9	23.3	15.7	12.3

B PDL	Activity (MBq/kg)	Time per bed position (s) EARL₂ 2mm					EARL₂ 4mm				
		30	60	120	180	300	30	60	120	180	300
T0	4	8.7	6.2	4.0	2.9	2.2	7.8	6.3	4.5	3.2	2.4
T0 + 1h	2.73	8.3	7.0	3.4	2.9	2.5	12.4	5.9	4.1	3.0	2.5
T0 + 2h	1.87	8.3	7.5	5.6	4.6	3.0	13.6	7.7	5.6	4.5	3.0
T0 + 3h	1.29	14.4	8.5	6.0	5.0	4.4	18.0	10.1	6.1	4.8	4.2
T0 + 4h	0.88	14.3	10.2	6.8	5.6	4.2	22.8	13.4	6.5	5.2	4.1
T0 + 5h	0.56	20.5	12.2	10.9	8.6	6.2	34.0	15.2	12.8	9.3	6.4
T0 +6h	0.41	23.5	17.8	9.0	9.1	7.3	49.9	29.5	13.2	10.0	7.4
T0 + 7h	0.28	37.3	19.1	11.9	11.2	8.5	69.7	40.0	16.3	10.6	8.5

COV ≤ 15 All recovery coefficients comply to accreditation specifications

COV ≤ 15 One or more spheres fall outside the accreditation specifications for SUV mean, maximum and/or peak activity concentration recovery coefficients

COV > 15

Figure 3. $EARL_1$ and $EARL_2$ (2 mm and 4 mm) compliance illustrating coefficient of variation (COV) at various [18F]FDG activity dosages and scan durations for reconstructions without (A) and with (B) precision deep learning image enhancement (PDL). SUV: standardized uptake value.

DISCUSSION

This phantom study provides an initial insight into the applicable lower limit in [18F]FDG administered activity and/or scan time reduction while being $EARL_1$ and $EARL_2$ Fluorine-18 compliant for the Omni Legend PET/CT system. Despite the larger voxel size, $EARL_2$ (4 mm) COV data were higher overall than $EARL_2$ (2 mm), which may be attributed to the higher beta value used in the 2 mm BPL reconstruction. Moreover, using the same method to assess reduction in administered activity, van Sluis et al. reported factors of reductions in administered activity at 1 min/bed of ~8 ($EARL_1$), ~4 ($EARL_2$, 4 mm) and 1 ($EARL_2$, 2 mm), where our results gave factors ~4, ~8 and ~4, respectively [13]. This difference can be explained by their use of a different scanner and reconstruction algorithms. Furthermore, our data show comparable findings for $EARL_2$ 2 mm on the Omni Legend system compared to Kennedy et al. (0.88 for our study compared to 1 $MBq \cdot min \cdot bed^{-1} \cdot kg^{-1}$ for Kennedy et al), yet scan times and reduction in administered activity are less thoroughly covered in their study [5]. Note that each institution is advised to explore different reconstruction parameters of their scanner to ensure EARL compliance with our indicated reductions in administered activity.

Our study has limitations. First, the NEMA IEC body phantom only simulates a 75 kg patient. Preferably, the validation should be replicated using phantoms simulating various patient sizes [14]. Second, we used one strategy to assess the reduction in administered activity, however, alternative methods are available to assess reduction in administered activity [15-18]. Third, this phantom does not reflect real-world conditions. Ideally, for future work we recommend that a clinical study should be performed to validate the image quality, the potential role of deep learning-enhanced post-processing and quantitative accuracy using [^{18}F]FDG PET data of patients scanned at the chosen lower regime in administered activity and/or reduced scan times. Note that the identified lower limits of [^{18}F]FDG administered activity only apply to the Omni Legend 32 cm PET/CT and that new studies should be performed to investigate the lower limits of [^{18}F]FDG administered activity for other PET systems.

In conclusion, we demonstrate in this phantom study that a reduction in [^{18}F]FDG administered activity is possible by at least a factor 4 for 1 min/bed with the Omni Legend 32 cm PET/CT while maintaining $EARL_1$ and $EARL_2$ compliance. A clinical study should be performed to validate these findings.

REFERENCES

1. von Schulthess GK, Steinert HC, Hany TF. Integrated PET/CT: current applications and future directions. Radiology. 2006;238:405-22.
2. Singh M. A review of digital PET-CT technology: comparing performance parameters in SiPM integrated digital PET-CT systems. Radiography (Lond). 2024;30:13-20.
3. Association NEM, Association NEM. NEMA standards publication NU 2–2018: performance measurements of Positron emission tomographs. National Electrical Manufacturers Association. 2018.
4. Smith RL, Bartley L, O'Callaghan C, Haberska L, Marshall C. NEMA NU 2-2018 evaluation and image quality optimization of a new generation digital 32-cm axial field-of-view Omni Legend PET-CT using a genetic evolutionary algorithm. Biomedi Phys Eng Express. 2024;10:025032.
5. Kennedy JA, Palchan-Hazan T, Maronnier Q, Caselles O, Courbon F, Levy M, et al. An extended bore length solid-state digital-BGO PET/CT system: design, preliminary experience, and performance characteristics. Eur J Nucl Medi Mol Imaging. 2024;51:954-64.
6. Yamagishi S, Miwa K, Kamitaki S, Anraku K, Sato S, Yamao T, et al. Performance Characteristics of a New-Generation Digital Bismuth Germanium Oxide PET/CT System, Omni Legend 32, According to NEMA NU 2-2018 Standards. J Nucl Med. 2023;64:1990-7.
7. Mehranian A, Wollenweber SD, Walker MD, Bradley KM, Fielding PA, Huellner M, et al. Deep learning–based time-of-flight (ToF) image enhancement of non-ToF PET scans. Eur J Nucl Med Mol Imaging. 2022;49:3740-9.
8. Kaalep A, Sera T, Rijnsdorp S, Yaqub M, Talsma A, Lodge MA, et al. Feasibility of state of the art PET/CT systems performance harmonisation. Eur J Nucl Med Mol Imaging. 2018;45:1344-61.
9. Boellaard R, Delgado-Bolton R, Oyen WJ, Giammarile F, Tatsch K, Eschner W, et al. FDG PET/CT: EANM procedure guidelines for tumour imaging: version 2.0. Eur J Nucl Med Mol imaging. 2015;42:328-54.
10. Boellaard R, Willemsen A, Arends B, Visser E. EARL procedure for assessing PET/CT system specific patient FDG activity preparations for quantitative FDG PET/CT studies. Last Accessed Sept [Internet]. 2014 2018.
11. Manual for EARL FDG-PET/CT Accreditation: Version 4.2. Vienna, Austria: EANM Research Ltd.;.March 2017.
12. Boellaard R. Quantitative oncology molecular analysis suite: ACCURATE. J Nucl Med. 2018.
13. Van Sluis J, De Jong J, Schaar J, Noordzij W, Van Snick P, Dierckx R, et al. Performance characteristics of the digital biograph vision PET/CT system. J Nucl Med. 2019;60:1031-6.
14. Peters SM, van der Werf NR, Segbers M, van Velden FH, Wierts R, Blokland KA, et al. Towards standardization of absolute SPECT/CT quantification: a multi-center and multi-vendor phantom study. EJNMMI Phys. 2019;6:1-14.
15. de Groot EH, Post N, Boellaard R, Wagenaar NR, Willemsen AT, van Dalen JA. Optimized dose regimen for whole-body FDG-PET imaging. EJNMMI Res. 2013;3:1-11.
16. Wickham F, McMeekin H, Burniston M, McCool D, Pencharz D, Skillen A, et al. Patient-specific optimisation of administered activity and acquisition times for 18 F-FDG PET imaging. EJNMMI Res. 2017;7:1-11.

17. Prieto E, García-Velloso MJ, Rodríguez-Fraile M, Morán V, García-García B, Guillén F, et al. Significant dose reduction is feasible in FDG PET/CT protocols without compromising diagnostic quality. Phys Med. 2018;46:134-9.

18. Katsari K, Penna D, Arena V, Polverari G, Ianniello A, Italiano D, et al. Artificial intelligence for reduced dose 18F-FDG PET examinations: a real-world deployment through a standardized framework and business case assessment. EJNMMI Phys. 2021;8:1-15.